Bulletin of the Seismological Society of America, Vol. 74, No. 1, pp. 167–179, February 1984

STUDY OF THE 6 JUNE 1977 LORCA (SPAIN) EARTHQUAKE AND ITS AFTERSHOCK SEQUENCE

BY J. MEZCUA, M. HERRAIZ, AND E. BUFORN

ABSTRACT

On 2 May 1977, a portable array of five stations was installed for the reconnaisance of the Alhama de Murcia fault in southern Spain. During this survey on 6 June 1977, a 4.2 m_b (*Lg*) shock took place within the array and was followed by a long series of aftershocks. Due to the good quality of the records, a comprehensive study of location, magnitude, seismic moment, focal mechanism, and related parameters has been carried out. In the seismic moment calculation, we have used the coda wave analysis, which also gives information about Q values of approximately 320 and 617 for body and surface waves, respectively. In evaluating the focal mechanisms of the sequence, we have used a joint treatment which permits us to separate the two types of faulting involved in the rupture process. Finally, to interpret these results in terms of the tectonics of the region, the focal mechanism of the earthquake of 5 March 1981, which occurred in a neighboring area, has also been studied.

INTRODUCTION

The study of seismically active faults is of great importance in the determination of seismogenic zones and critical in assessing the seismic risk of a given area. The spatial correlation between seismicity and geologically mapped faults requires very precise epicentral determinations. This can only be accomplished in regions where dense seismological networks are in operation, which is not the case for most regions, especially those of moderate seismicity. To correct this situation, portable stations must be used in temporary seismic arrays. This was done for a study of the Alhama de Murcia fault in southeast Spain, where a seismic survey was carried out during the period between 2 May and 2 July 1977 with five portable seismic stations. During this survey, on 6 June 1977, a 4.2 m_b (*Lg*) shock took place in the vicinity of the array, and was followed by a long series of aftershocks. This series was recorded by the portable array, allowing a very precise analysis of its characteristics. This analysis includes the spatial and temporal distribution of the aftershocks, their focal mechanisms, the mean Q values of the zone, and a moment-magnitude relationship.

TECTONIC FRAMEWORK AND SEISMICITY OF SOUTHERN SPAIN

The main structural elements of the southern part of the Iberian Peninsula are summarized in Figure 1. The most recent tectonic episode corresponds to the Alpine orogeny in the Betic Cordillera, in which, depending on the materials affected, two different domains may be considered. The External zone is formed of Mesozoic and Tertiary materials, whereas the Internal or Betic zone is composed of Triassic and older rocks (Egeler and Fontboté, 1976). In the eastern part of the Betic Cordillera, two different tectonic periods are found (Bousquet and Montenant, 1974a, b; Bousquet and Philip, 1976) during most recent time. In the older one, from the Tortonian through Pliocene, the area was affected by normal faulting with NE–SW trends, followed by an episode, during the middle and present Quaternary, charac-

terized by compressional features extending through the Alboran Sea (The Research Group of Neotectonic in the Gibraltar Arc, 1977).

In the more recent tectonic period, the normal faults of the tensional stage have been reactivated either as reverse fault striking in the E–W direction or strike slip faults in a direction N40°E–N60°E (Armijo *et al.*, 1977). One of the most important is the Alhama de Murcia fault with a total length of about 100 km and N55°E

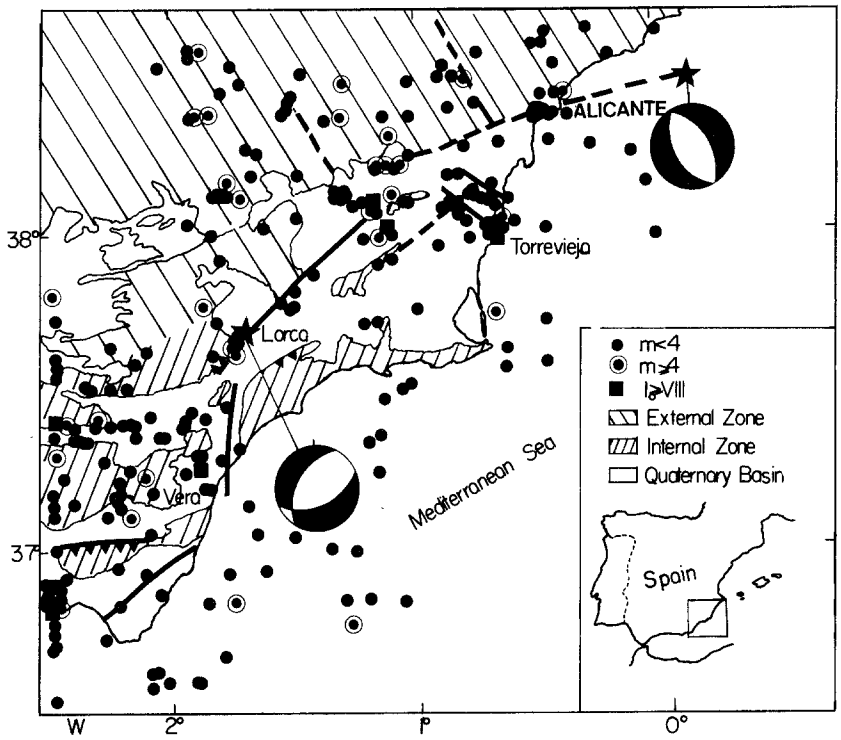

FIG. 1. Tectonic map southern Spain showing the main structural elements and the seismicity of the area. Historical events with maximum intensity $I_0 \geqq VIII$ are shown together with the instrumental seismicity for the period 1940 to 1980. Focal mechanisms of 6 June 1977 Lorca earthquake and the shock on 1 March 1981 (east of Alicante) are also included.

strike. The southern end of this fault, which is near Lorca, continues to have tensional faulting. The amount of slip during the Quaternary is not known because facies of Upper Miocene deposits are only locally different on both sides of the fault (Bousquet, 1979). However, if this fault is considered to have strike-slip movement, the total offset can be inferred from the main tectonic contact between the Internal and External zones of the Betic Cordillera, being a horizontal displacement of the order 60 km (Bousquet, 1979).

In Figure 1 are also shown the epicenters of earthquakes, taken from the Catalogue of the Spanish Seismological Service (SSIS), for the southeastern part of Spain. Historial events with intensity $I_0 \geqq$ VIII are shown, together with the instrumental epicenters for the period 1940 to 1980. A relocation of epicenters for the period 1955 to 1980 has been done, making use of an average velocity structure obtained from deep seismic reverse profiles in the area (Banda *et al.*, 1983).

Epicenters of some of the major shocks lie near the main mapped faults for the area. To the north, passing through Alicante, there is an epicentral alignment (dashed line in Figure 1) in the NE–SW direction which is interpreted as a continuation of the Alhama de Murcia fault. Over this line is located the 5 March 1981 earthquake, whose focal mechanism is also given, and is located at the northeast end of the line. At about 38°N, 1°W there are two strike-slip faults with a NW–SE trend that follow the pattern of seismicity. One of these earthquakes was the Torrevieja earthquake of 29 March 1829 with an assigned intensity of *X* (MSK). Further to the south and west, the Alhama de Murcia fault, which has a NE–SW strike direction, does not have many events associated with it, except near Lorca where several shocks, including the 1977 Lorca earthquake, have epicenters near the fault.

South of Lorca, there is a N–S striking fault which may be related to the Vera earthquake in 1518 of intensity *X*, but few instrumental epicenters seem to be associated with the fault. This fault has been described also as a possible continuation to the south of the Alhama de Murcia fault system (Bousquet and Montenant, 1974a).

As may be noticed, the diffuse patterns of epicenters make it very difficult to relate the earthquake activity with the faults. An explanation might be the lack of accuracy in location parameters, due to a poor azimuthal coverage by the permanent seismic network.

The 6 June 1977 Lorca Earthquake

On 2 May 1977, an array of five portable stations (MEQ-800) was installed in the area near Lorca. The distribution of stations is shown in Figure 2. Coordinates and dates of operation are listed in Table 1. The time of each internal clock was daily calibrated by use of the time signals from the DCF (77 kHz) station in Germany. During the operation of the network, prior to the 6 June, the occurrence of earthquakes was moderate with about one shock/day. Their epicenters were located mainly to the southeast of the Alhama de Murcia fault, with the exception of one shock (m = 0.5) on 1 June, at 23:58, that may be considered as a foreshock. On 6 June 1977 at 10:49:12.7 UTC, occurred the main shock of magnitude m (L_g) = 4.2, that was felt over 3.000 km^2 area and has a maximum intensity of VI (MSK). The epicenter lies very close to the Alhama de Murcia fault. Because the main shock was followed by a large number of aftershocks, the survey was continued until 2 July, when the aftershock activity dropped down to less than one shock/day.

The hypocenter of the main shock was independently calculated by using two sets of data. One came from the portable network. The other made use of data of the Spanish network supplemented with data from stations in Portugal, Morocco, Algeria, and France. The final parameters, calculated by using HYPO 71 (Lee and Lahr, 1975) are given in Table 2, together with solutions given by different agencies. As can be observed, the differences in epicentral coordinates and depth are no greater than about 25 km.

Focal mechanism and parameters. To study the focal mechanism, *P* onset polarities from 22 stations were read. For those within a very close distance (*Pg* range), up to 100 km, the take-off angle was derived from the velocity structure of the zone and adjusted to a linear velocity increase with depth. For larger distances, the J-B tables were used. Using the methodology and computer program described by Udias

et al. (1982), the focal mechanism of the main shock was calculated. The solution is shown in Figure 1, and the values of its parameters and standard deviations are listed in Table 3.

The score of the solutions is $p = 0.91$, and the standard deviation of the strike of

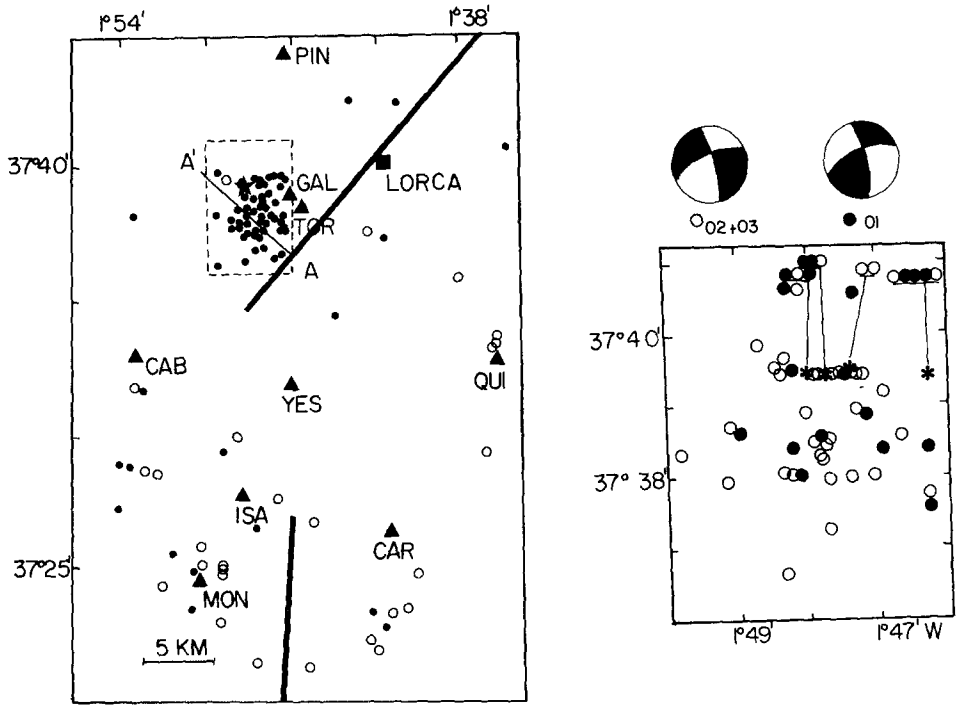

FIG. 2. (*Left*) Epicenters previous to the main shock (open circles) and main event (star) and aftershock sequence (solid circles) of the 6 June 1977 Lorca earthquake. Stations of the temporary array are indicated by triangles. Also shown is the Alhama de Murcia fault trace. (*Right*) Enlarged view of the dashed line rectangle, with the distribution of the sequence used in the joint focal mechanism. Solid circles represent those shocks having reverse faulting and open circles those with normal faulting. Stars represent groups of aftershocks with the same epicentral coordinates.

TABLE 1

LOCATION OF SEISMIC STATIONS

Station Code	Latitude (N)	Longitude (W)	Date of Operation
PIN	37°44.90′	1°46.07′	22 June–2 July
GAL	37°39.33′	1°46.37′	26 May–2 July
TOR	37°38.80′	1°45.67′	22 May–25 May
CAB	37°33.10′	1°54.17′	22 May–2 July
YES	37°31.95′	1°46.52′	2 May–22 May
QUI	37°32.93′	1°36.44′	2 May–2 July
CAR	37°26.45′	1°41.44′	2 May–22 June
MON	37°24.58′	1°50.66′	15 May–2 July

the selected nodal plane is 12°. The mechanism correspond to normal faulting, with the tension axis horizontal and trending NW–SE. Both planes indicate predominant dip-slip motion, and their strikes coincide roughly the trace of the Alhama de Murcia fault. This fault, however, has been interpreted on geological grounds as a

strike-slip fault with left-lateral motion (Bousquet, 1979). But, as we will see later, a mechanism with predominant normal faulting also results from the joint analysis of the aftershock sequence.

Short-period P and S waves, recorded by four well-calibrated stations, were digitized and Fourier analyzed to obtain a log–log plot of spectral amplitude and frequency. Using Brune's model, a seismic moment of 5.71×10^{22} dyne-cm and a radius of the equivalent dislocation of 3.2 km were deduced (Herraiz and Mezcua, 1979). This result agrees reasonably well with the estimation derived from the aftershock area of 56 km^2.

TABLE 2

MAIN EVENT SOLUTIONS

Agency*	Origin Time	Latitude	Longitude	Depth	Magnitude
CSEM	10 49 12.3	37.62	1.88	10	
ISC	10 49 10.2 ± 26	37.66 ± 030N	1.83 ± 036W	10	4.1*b*
LDG	10 49 14.9	37.70	1.80	35	4.2*L*
NEIS	10 49 12.7	37.80	1.80	33	4.2b 3.8*S*
SSIS	10 49 09.5	37.70	1.80	10	4.2 m_b (*Lg*)

* CSEM, Centre Sismologique Europeo-Mediterraneen, Strasbourg, France; ISC, International Seismological Centre, Newbury, England; LDG, Laboratorie de Détection et de Géophysique, Paris, France; NEIS, National Earthquake Information Service, Boulder, Colorado; and SSIS, Sección de Sismología e Ingeniería Sísmica, Madrid, Spain.

TABLE 3

FOCAL MECHANISM SOLUTIONS*

	θ	Φ	ϕ	δ	λ	P
5 March 1981	*T*: 83° ± 5°	251° ± 15°	*A*: 336° ± 41°	44° ± 3°	84° ± 73°	0.70
(Mediterranean Sea)	*P*: 5° ± 11°	141° ± 77°	*B*: 165° ± 8°	47° ± 5°	84° ± 62°	
6 June 1977	*T*: 86° ± 2°	140° ± 6°	*A*: 208° ± 14°	45° ± 2°	57° ± 10°	0.91
(Lorca)	*P*: 23° ± 5°	40° ± 6°	*B*: 70° ± 12°	53° ± 6°	61° ± 5°	
Lorca 1	*T*: 58° ± 10°	213° ± 9°	*A*: 249° ± 12°	57° ± 4°	14° ± 14°	0.72
(21 shocks)	*P*: 76° ± 10°	114° ± 1°	*B*: 347° ± 6°	78° ± 10°	34° ± 2°	
Lorca 2	*T*: 69° ± 15°	112° ± 9°	*A*: 248° ± 35°	44° ± 10°	18° ± 45°	0.70
(19 shocks)	*P*: 49° ± 6°	222° ± 17°	*B*: 351° ± 16°	78° ± 35°	48° ± 3°	
Lorca 3	*T*: 79° ± 8°	112° ± 2°	*A*: 244° ± 18°	57° ± 26°	19° ± 33°	0.86
(25 shocks)	*P*: 55° ± 4°	209° ± 5°	*B*: 345° ± 12°	74° ± 30°	34° ± 11°	

* θ, 90°-plunge; Φ, azimuth angle; ϕ, δ, λ, strike, dip, and slip angle; P, total score or proportion of consistencies.

As mentioned before, an earthquake of m_b (*Lg*) = 4.8 took place at 38°49N, 0.13°E on 5 March 1981, 01h21m (Figure 1). This shock is possibly related to the same fault system, further north of Lorca, as described before. The mechanism is also of normal type with horizontal T axis in the NE–SW direction. The values of parameters of the nodal planes are given in the first row of Table 3. The solution is based on 43 P observations, and the score is $p = 0.70$. This shock has been taken into account in the tectonic interpretation of the Lorca earthquake.

STUDY OF THE AFTERSHOCK SEQUENCE OF THE LORCA EARTHQUAKE

Location. Location, origin time, and depth of aftershocks were determined using the HYPO 71 program, (Lee and Lahr, 1975) with the velocity structure obtained

for this area (Banda and Ansorge, 1980). In order to minimize the effects of abrupt discontinuities in P velocity, the upper layers were smoothed. For the S-wave velocity structure, a ratio $V_P/V_S = 1.72$ with extreme values of 1.63 and 1.88 was used in light of the Wadati diagram calculated for those shocks with clear S onsets. Taking a minimum number of observations equal to four for at least three stations, a total of 119 epicenters were calculated. These minimum requirements correspond to an average magnitude of 0.5. Figure 2 (*left*) shows the epicenters of the earthquakes that occurred in the month previous to the main shock (open circles). In the same figure, a sketch of the observed trace of the Alhuma de Murcia fault, and its possible continuation to the south, is also included. It is clear that the events that occurred before 6 June are concentrated mainly in the southeast near the stations of MON and CAR. Some of the smaller events, however, may be quarry blasts. Only

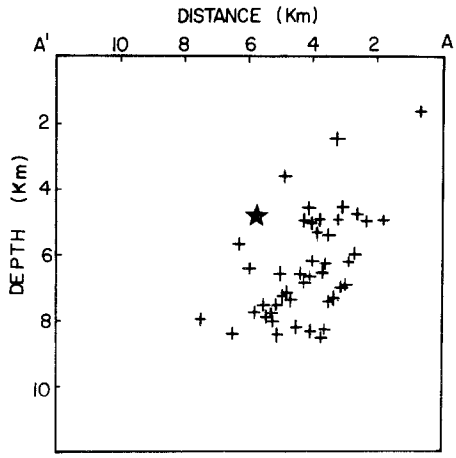

FIG. 3. Vertical section of the best-determined foci of the aftershock sequence projected on plane $A - A'$ perpendicular to the fault trace.

one foreshock, 5 days before, was located close to the 6 June main shock. In relation to the aftershock sequence, it can be observed that most of the shocks are clustered west of the fault. The depth control was in general rather poor due to the small number of stations. In spite of all the limitations, a trial depth of 5 km seems to provide a good fit to the data. As can be observed, the main shock and aftershocks cluster approximately 5 km northwest of the fault, with no clear alignment along the fault's trace. This is believed to be caused by epicentral mislocation, resulting from lateral inhomogeneity detected on seismic profiles carried out in this specific area.

A selection of 50 of the better-located aftershocks was projected onto a vertical plane perpendicular to the fault strike (Figure 3). The 45° dip to the northwest, obtained from the focal mechanism solution for plane A, agrees with the dip of the aftershock plane. The cluster at 6- to 8-km depth may be an indication of the correct focal depth of the main shock.

Magnitude distribution. A formula for magnitude based on duration was developed for this area, following Lee *et al.* (1972). The constants of the magnitude-duration formula were derived by using the magnitude values obtained for Toledo station, where three aftershocks with clear *Lg* waves were recorded. The final expression is

$$m_\tau = -2.10 + 2.89 \log \tau. \quad (1)$$

The duration magnitude, m_τ, of equation (1) gives magnitudes which are equivalent to the m_b (Lg) values adopted for the Spanish Catalogue. The distance term in the definition of m_τ has been omitted because of its small influence for the short distance range used.

Magnitude values obtained for the 58 shocks located prior to the event and for the aftershock sequence were used to determine the b values of the m versus log N relationship (Figure 4). For the preevent shocks, a value of $b = 0.58 + 0.02$ was found, while for the aftershocks it was 0.67 ± 0.02. The b variation, if the main event is removed and the adjustment is less than 5 per cent, which corresponds to results obtained for other sequences (Morrison *et al.*, 1976). The small difference in the value of b obtained for the preevent activity and the following sequence question the use of changes in this parameter as a premonitory index.

Temporal distribution. The located aftershocks were fitted to the Omori's relation $\log N(t) = K\text{-plog}\ (t + c)$, where N is the number of events/unit time and K the activity factor. A time interval of 20 hr was selected for the analysis. The least-

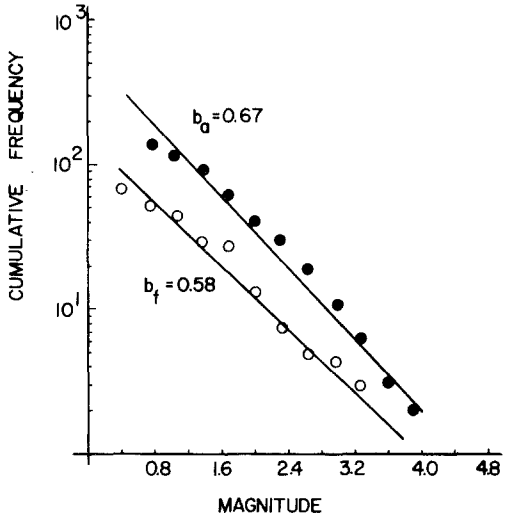

FIG. 4. Cumulative frequency versus magnitude plot for the foreshock (open circles) and aftershock (solid circles) sequences.

squares value for K is 1.05, which is of the same order as those found in Japan (Utsu, 1961) but larger than those found for the Oroville earthquake sequence of August 1975 (0.70) (Morrison *et al.*, 1976) and for the aftershocks of the Friuli earthquake of 6 May 1976 (0.85) (Mayer-Rosa *et al.*, 1977).

CODA ANALYSIS OF THE AFTERSHOCKS

While most of the coda wave analysis has been performed with digital data (Aki, 1969), in this case only visible recordings were available. This type of data creates many problems, some arising because of the limited frequency band, which makes the conclusions more restricted. The generation model for coda waves selected is the "single scattering" one (Aki and Chouet, 1975) in which both body and surface waves are considered as responsible for the origin of the coda. Following Aki and Chouet (1975), the power spectrum of the coda waves is written as

$$P(\omega, t) = S(\omega)t^{-m}e^{-\omega T/Q}, \tag{2}$$

where $S(\omega)$ represents the effect of the earthquake source, t the time since origin of the shock, m is a constant determined by the geometrical spreading (2 for body waves and 1 for surface waves), and Q the quality factor. Relating the power spectrum $P(\omega, t)$ with the amplitudes A_i at an instant of time t_i, and extending for j earthquakes of the same area, we obtain

$$\log A_{ij}(\omega, t) = C_j(\omega) - \frac{m}{2} \log t_i - bt_i \tag{3}$$

where C_j depends on $S(\omega)$, and $b = \log e^{\omega/2Q}$.

This expression has been applied in order to obtain the value of Q and $S(\omega)$ by using 22 aftershocks in the magnitude range $1.7 < m_\tau < 3.5$ and focal depth varying between $1 < h < 15$ km (Herraiz, 1982). After applying a least-squares inversion, the results obtained at a mean frequency of 5 Hz for Q are 320 ± 43 and 617 ± 99 for surface waves and body waves, respectively. Because this study is frequency-fixed, it was not possible to examine the frequency dependence of Q. The value of Q fit reasonably well with those of other regions in this frequency range. Values for $C_j(\omega)$ correlated very well with magnitudes, as should be expected due to the close relationship between magnitude and the process at the earthquake source.

If we restrict ourselves to the model in which scattering of surface waves is the only mechanism responsible for the generation of the coda, we can write the "reduced coda spectrum" (Aki, 1969) as

$$M_0 R_{SF} = t^{1/2} e^{\omega \cdot t/2Q} \cdot \left(\frac{-1}{Q} \frac{dt}{df}\right)^{1/4} \cdot A(\omega, t) \tag{4}$$

where M_0 is the seismic moment, R_{SF} is the "regional scattering factor", and dt/df is the variation with time of the peak frequency. This expression has been used to determine M_0 and R_{SF} once dt/df and Q are known. From the calculation of dt/df, $\log f = 0.877 - 0.004\ t$. To calibrate expression (4), we need an independent determination of the value of M_0. For this, we use the shock of 9 June 1977 at 08:17:22 (UTC) which was very well recorded in several stations of the Spanish network. Using the spectra of P and S waves, we found for this event a seismic moment of $2.81 \cdot 10^{20}$ dyne-cm. From this value, together with the Q calculated above, and the corresponding dt/df, a value for the "regional scattering factor" R_{SF} of $3.5\ 10^{-27}$ cm · sec/dyne-cm was reduced for the area. This R_{FS} value, common to the entire area, was substituted in expression (4) to obtain values of seismic moments for 21 aftershocks.

Finally, a correlation of the seismic moments with magnitude was made, giving

$$\log M_0 = (16.15 \pm 0.05) + (1.23 \pm 0.02)M. \tag{5}$$

The data are presented in Figure 5, M being the duration magnitude defined above.

If we compare this relationship with those obtained for local shocks by other authors, we find that it is very similar to those of Thacher and Hanks (1973), Bakun *et al.* (1976), and Modiano (1980). Also presented in Figure 5 are the lines corresponding to constant apparent stress, σ_a. We can see that, on the average, the observed values fit reasonably well with the line corresponding to $\sigma_a = 10$ bars. However, a linear decrease of σ_a with smaller magnitudes is apparent, which may

be an indication of the variation of the relative strength of the material at the focal region. Very small earthquakes may be affected by local low strength volumes of rocks in the upper crust.

JOINT FOCAL MECHANISM OF THE AFTERSHOCKS

Data from 65 aftershocks in the magnitude range $1 < m_r < 4$, which were observed at least at three stations, have been used in a joint treatment according to the technique given in Udias *et al.* (1982). In Figure 6, the successive ρ_i versus p_i plots of the process of separation of the aftershocks into three groups are shown. The

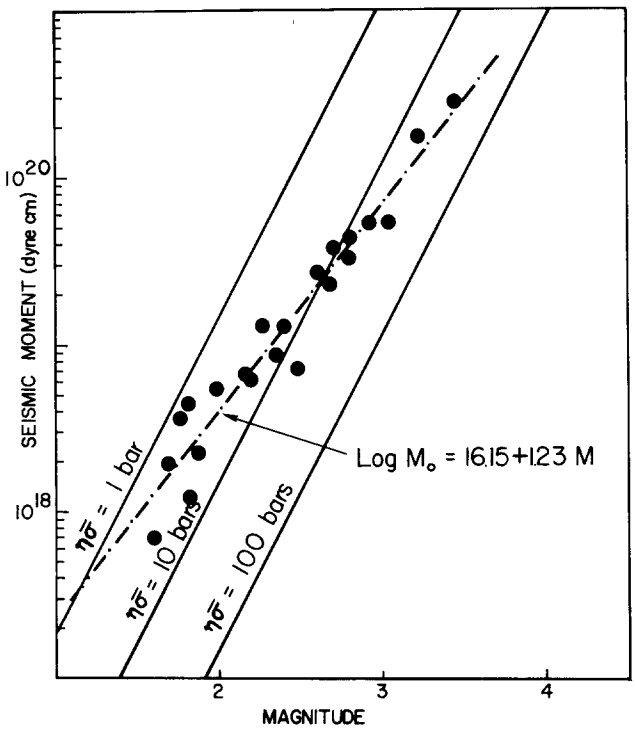

FIG. 5. Relation between seismic moment and magnitude. The straight lines are those for constant apparent stress. Dashed line corresponds to the least-squares fit calculated for the Lorca earthquake sequence.

parameter ρ_i, as defined in the forementioned paper, weighs the data of each event according to its agreement with the group solution, and p_i is the score of the solution (correct over total number of observations). Separation into groups of events is based on the comparison of the individual scores p_i with a selected threshold value. In this case, the first division was made according to the positive or negative values of p_i. In this first division, two mechanisms are found corresponding to normal (44 events) and reverse faults (21 events). The normal fault mechanism is further subdivided into two groups, using the threshold value of $p = 0.75$ (see Figure 6). Consequently, three groups are found, two corresponding to normal (2 and 3) and one (1) to reverse faulting. Orientation of the nodal planes for the joint solutions of the three groups, number of events, and total number of observations for each group are given in Table 3. The solution and data for group 3 are presented in Figure 7.

The orientation of the nodal planes of groups 2 and 3, consisting of a total of 44 events, indicates normal faulting of very similar character. However, the groups are divided according to the value of the score p (0.70 for group 2 and 0.86 for group 3). Group 1 corresponds to reverse faulting ($p = 0.72$) and includes 21 events.

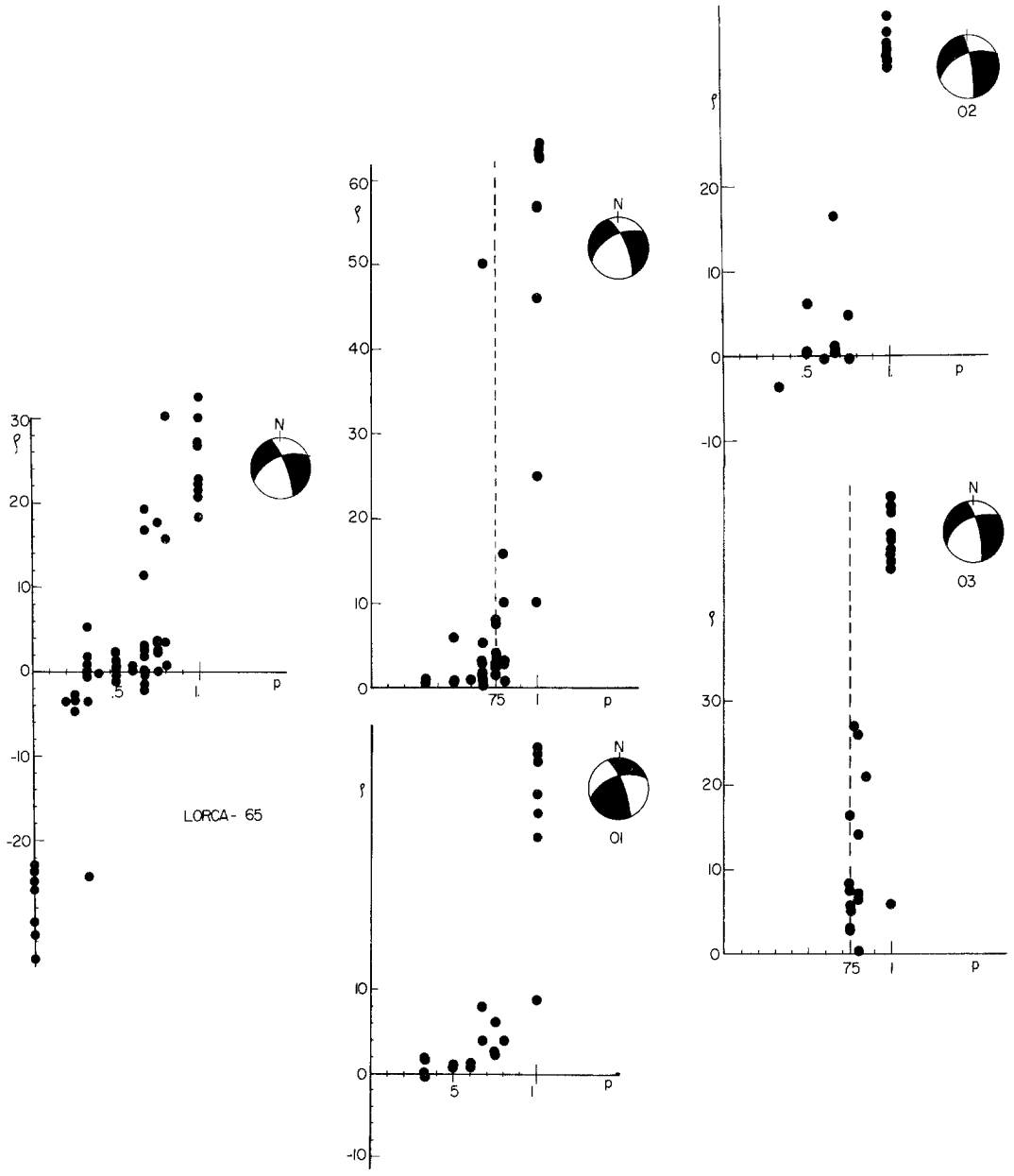

FIG. 6. Plots of p_i versus ρ_i for the 65 selected aftershocks. Joint solution and the process of separation into positive and negative values of ρ is shown.

The spatial distribution of the epicenters with normal or reverse mechanism is shown in Figure 2. There is no apparent pattern present, but this may be due to the lack of precision in the epicentral determinations.

The temporal distribution of the sequence of normal and reverse mechanism as

a function of magnitude is shown in Figure 8. Most shocks with magnitudes greater than or equal to 2 are of normal character (only three exceptions), but a definite pattern of alternating mechanism with time does not seem to be present.

The mechanisms of the main shock and more than two-thirds of the aftershocks studied correspond to a normal fault which strikes more or less in the direction of

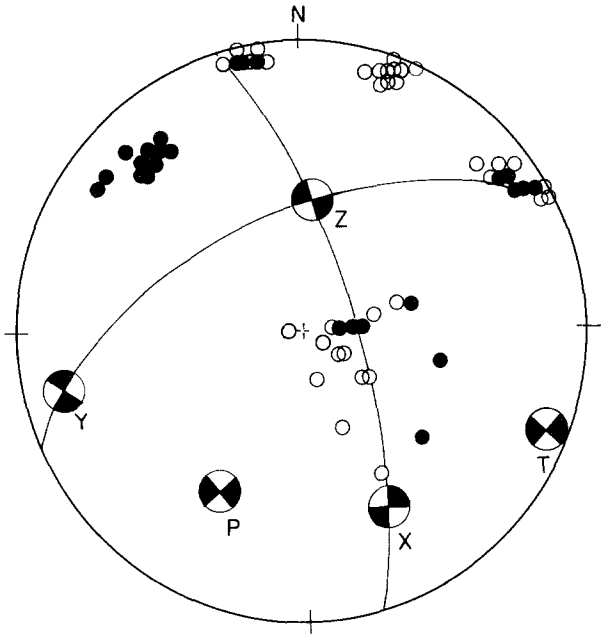

FIG. 7. Composite focal mechanism solution for group 3 of the Lorca earthquake sequence. Solid circles represent compressions and open circles dilatations.

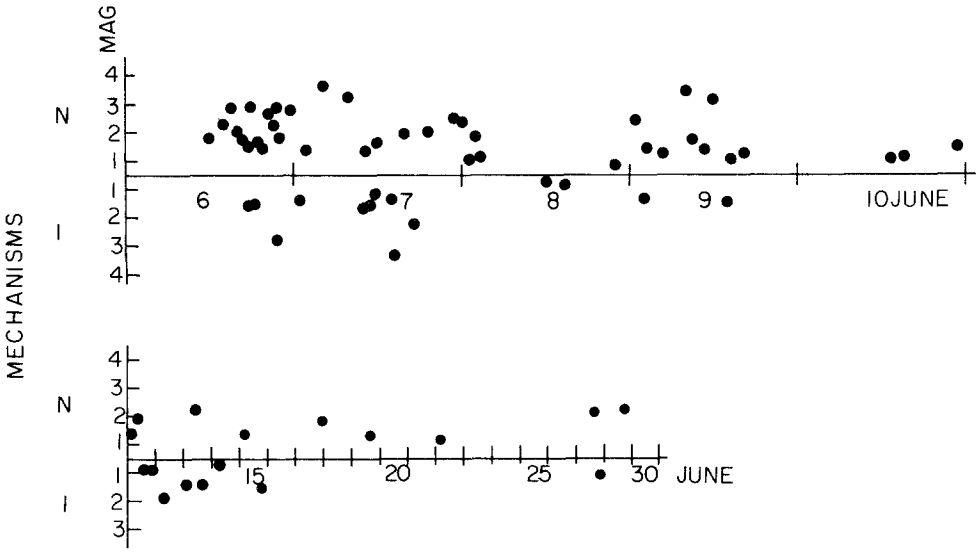

FIG. 8. Temporal distribution of the focal mechanism as a function of magnitude. (N) indicates normal and (I) reverse faulting. The *upper part* corresponds to the first 5-day period and the *bottom* to the next 20 days.

the Alhama de Murcia fault, with the T axis horizontal and having a NW–SE direction. One-third of the aftershocks, however, had a mechanism of the opposite type, i.e., of reverse character. This result may be interpreted as a rebound motion along the same plane of fracture.

Conclusions

The location of the main event and aftershocks of the Lorca 6 June 1977 earthquake suggests a relationship with the Alhama de Murcia fault, thus characterizing it as an active fault. The offset of the epicenters of the aftershock sequence with the trace of the fault is interpreted on basis of depth distribution of the events, contained in an approximately 45° dip plane, and uncertainty in the velocity structure. The orientation and dip of such a plane coincides with one of the planes deduced for the focal mechanism of the main shock. The earthquake of 5 March 1981, with also a normal focal mechanism, seems to be associated with a fault which is interpreted as a continuation to the north of the Alhama de Murcia fault. These two earthquakes provide additional data in order to interpret the faulting processes of the area. While on geological grounds this fault is taken as a transcurrent fault, the focal mechanisms obtained indicate normal faulting. However, present-day activity could be a reactivation of an existing fault, but with a different stress regime. This apparent discrepancy makes it necessary to obtain more data in order to accomplish both tectonic and seismic information.

The b values calculated for the preevent and aftershock series are 0.58 and 0.67, respectively. This small diference in the b value is in accordance with what Knopoff *et al.* (1982) have found in other earthquake series. This small difference diminishes the predictive value of such a parameter. The temporal distribution of the aftershock sequence has an activity factor K of 1.05.

The joint treatment of the first-motion data of the aftershocks points out three different kinds of mechanisms. Two are of normal fault type in coincidence with the main shock mechanism and one is of the reverse type. The latter may be interpreted as the result of a rebound motion along the fracture plane. In the temporal distribution of bone mechanisms, there is no clear alternative change from normal to reverse motion.

The application of the coda wave analysis to the sequence yields regional values of Q for body and surface waves in the area of 617 and 320, respectively. Seismic moments deduced for each earthquake show a relation with magnitude which is in agreement with those calculated by other authors for a similar magnitude range. Average observed values agree with a constant apparent stress of about 10 bars, although at present, there seems to be a trend of diminishing stress with decreasing magnitudes.

Finally, the temporal distribution of the focal mechanisms for the aftershock sequence does not show any clear relationship beween magnitude and type of faulting.

Acknowledgments

The authors would like to express their appreciation to J. Galán and J. Revuelta for operating the network, and to the computer centers of Instituto Geográfico Nacional and Junta de Energía Nuclear of Madrid. We are also especially grateful to Professors Otto W. Nuttli and A. Udías for reading the manuscript and offering many helpful comments.

References

Aki, K. (1969). Analysis of the seismic coda of local earthquakes as scattered waves, *J. Geophys. Res.* **74**, 615–631.

Aki, K. and B. Chouet (1975). Origin of coda waves: source, attenuation and scattering effects, *J. Geophys. Res.* **80,** 3322–3342.

Armijo, R., J. Benkhelil, J. C. Bousquet, A. Estevez, R. Guiraud, C. Montenant, M. J. Pavillon, H. Philip, C. Sanz De Galdeano, and C. Viguier (1977). Les resultats de l'analyse structural en Espagne, *Bull Soc. Geol. Fr.* **XIX,** 591–605.

Banda, E. and J. Ansorge. (1980). Crustal structure under the central and eastern part of the Betic Cordillera, *Geophys. J. R. astr. Soc.* **63,** 515–532.

Banda, E., A. Udias, St. Mueller, J. Mezcua, M. Boloix, J. Gallart, and A. Aparicio (1983). Crustal structure beneath Spain from deep Seismic sounding experiments, *Phys. Earth Planet. Interiors* (in press).

Bakun, W., G. Bufe, and R. Stewart (1976). Body-wave spectra of central California earthquakes, *Bull. Seism. Soc. Am.* **66,** 363–384.

Bousquet, J. C. (1979). Quaternary strike-slip faults in Southeastern Spain, *Tectonophysics* **52,** 277–286.

Bousquet, J. C. and C. Montenant (1974a). Présence de decrochements Nord-Est–Sud-Oest quaternaries dans les Cordilleres Betiques Orientales (Espagne). Extension et signification generale, *C.R. Acad. Sci., Paris* **278,** 2617–2620.

Bousquet, J. C. and C. Montenant (1974b). La neotectonique dans les Cordilleres Betiques Orientales, Meeting Soc. Terre, Nancy, France, p. 81.

Bousquet, J. C. and H. Philip. (1976). Observations microtectoniques sur la compression Nord Sud quaternarie des Betiques Orientales (Espagne meridionale, Arc de Gibraltar), *Bull. Soc. Geol. Fr.* **3,** 711–724.

Egeler, C. G. and J. M. Fontoboté. (1976). Aperçu geologique sur les parties Centrales et Orientales des Cordilleres Betiques, *Bull. Soc. Geol. Fr.* **3,** 571–582.

Herraiz, M. (1982). Microsismicida en el campo próximo. Análisis de generación de ondas de coda y parámetros físicos asociados, *Tesis Doct. U. Complutense*, Madrid, Spain, 207 pp.

Herraiz, M. and J. Mezcua (1979). Aplicación del análisis espectral al sismo de Lorca del 6 de Junio de 1977. Determinación de los parámetros focales. III. Asam. Nac. Geod. y Geofísicia, Inst. Geogr. Nac. Madrid. 395–417.

Knopoff, L., Y. Y. Kagan, and R. Knopoff (1982). *b* Values for foreshocks and aftershocks in real and simulated earthquakes sequences, *Bull. Seism. Soc. Am.* **72,** 1663–1676.

Lee, W. and J. C. Lahr. (1975). HYPO 71: a computer program for determining hypocenter, magnitude and first motion pattern of Local earthquakes, *U.S. Geol. Surv., Open-File Rept.*, 114 pp.

Lee, W. H. K., R. E. Bennet, and K. L. Meagher (1972). A method of estimating magnitude of local earthquakes from signal duration, *U.S. Geol. Surv., Open-File Rept.*, 21 pp.

Mayer-Rosa, D., N. Pavoni, and R. Graf (1977). The Friuli earthquakes of May 6, 1976: a preliminary study of intensity-attenuation, aftershocks and focal mechanism, *Publ. Inst. Geophys. Pol. Acad. Sci.* **A-6** (117), 57–61.

Modiano, T. (1980). Sismotectonique des Pyrenees occidentales. Etude detaille du contenu spectral des ondes de volume dans la region focale, *These*, Université Sci. et Med., Grenoble, France, 188 pp.

Morrison, P. W., B. W. Stump, and R. Uhrhammer (1976). The Oroville earthquake sequence of August 1975, *Bull. Seism. Soc. Am.* **66,** 1065–1084.

Thatcher, W. and T. Hanks (1973). Source parameters of southern Californian earthquakes, *J. Geophys. Res.* **78,** 8547–8576.

Udias, A., E. Buforn, D. Brillinger, and B. Bolt (1982). Joint statistical determination of fault-plane parameters, *Phys. Earth. Planet. Interiors* **30,** 178–184.

Utsu, T. (1961). A statistical study on occurrence of aftershocks, *Geophys. Mag.* **3,** 521–616.

Research Group of Neotectonics of the Gibraltar Arc. (1977). L'historie tectonique recente (Tortonian a Quaternarie) de l'Arc de Gibraltar et des bordures de la Mer d'Alboran, *Bull. Soc. Geol. Fr.* **3,** 575–576.

INSTITUTO GEOGRAFICO NACIONAL
SECCION DE SISMOLOGIA
MADRID 3, SPAIN (J.M.)
CONTRIBUTION NO. 204

CATEDRA DE GEOFISICA
UNIVERSIDAD COMPLUTENSE
MADRID, SPAIN (M.H., E.B.)
CONTRIBUTION NO. 211

Manuscript received 9 May 1983